

REPORT DOCUMENTATION PAGE			Form Approved OMB NO. 0704-0188	
Public reporting burden for this collection of information is estimated to average 1 hour per response, including the time for reviewing instructions, searching existing data sources, gathering and maintaining the data needed, and completing and reviewing the collection of information. Send comment regarding this burden estimate or any other aspect of this collection of information, including suggestions for reducing this burden, to Washington Headquarters Services, Directorate for Information Operations and Reports, 1215 Jefferson Davis Highway, Suite 1204, Arlington, VA 22202-4302, and to the Office of Management and Budget, Paperwork Reduction Project (0704-0188), Washington, DC 20503.				
1. AGENCY USE ONLY (Leave blank)	2. REPORT DATE JANUARY 25, 1996	3. REPORT TYPE AND DATES COVERED Final 1 Jul 95 - 31 Dec 95		
4. TITLE AND SUBTITLE High-Frequency Planar Power Transformer for Switching Power Supplies		5. FUNDING NUMBERS DAAH04-95-1-0409		
6. AUTHOR(S) Hung Y. David Yang, Pervez Dalal, Ming Y. Ng, Tzung-Ta Kao, C.Q. Lee		8. PERFORMING ORGANIZATION REPORT NUMBER		
7. PERFORMING ORGANIZATION NAME(S) AND ADDRESS(ES) Dept. of Electrical Engineering and Computer Science, 1120 SEO, 851 S. Morgan St., Univ. of Illinois at Chicago Chicago, IL 60607-7053		10. SPONSORING / MONITORING AGENCY REPORT NUMBER ARO 34423.1-EL-II		
9. SPONSORING / MONITORING AGENCY NAME(S) AND ADDRESS(ES) U.S. Army Research Office P.O. Box 12211 Research Triangle Park, NC 27709-2211		11. SUPPLEMENTARY NOTES The views, opinions and/or findings contained in this report are those of the author(s) and should not be construed as an official Department of the Army position, policy or decision, unless so designated by other documentation.		
12a. DISTRIBUTION / AVAILABILITY STATEMENT Approved for public release; distribution unlimited.				
13. ABSTRACT (Maximum 200 words) In this project, we proposed novel transformers for power supplies. Transformers consists of cascade of sections of transmission lines, each a quarter-wave length long at the design frequency. Power conversion is through the propagation of electromagnetic waves instead of magnetic flux. Parallel strip lines sandwiching a printed circuit board were used as the transmission lines. Printed meandered striplines on a multi-layer structure were used to optimize the component size. Three printed stripline transformers are built on Teflon-fiberglass for a hundred MHz applications. S parameter tests for a 50 ohm load show the measured transformer ratio agrees excellently with the prediction. The overall efficiency is greater than 98% due to very low material losses. A transformer is also built on a lead Zirconate Titanate material with dielectric constant 1100 at 8 MHz. 40 cm quarter-wave strip lines are built on a 3.1 inch by 3.1 inch plate. Open-circuit and short-circuit tests on network analyzer show the actual quarter-wave length is at 8.3 MHz instead and the line impedance (4Ω) also agrees well with the design value (4.4Ω). The S parameter measurement of the transformer ratio does not show good results, however, due to high material losses.				
14. SUBJECT TERMS Planar Transformer, Transmission lines, Strip Lines, Integrated Circuits		15. NUMBER OF PAGES 37		16. PRICE CODE
17. SECURITY CLASSIFICATION OR REPORT UNCLASSIFIED	18. SECURITY CLASSIFICATION OF THIS PAGE UNCLASSIFIED	19. SECURITY CLASSIFICATION OF ABSTRACT UNCLASSIFIED	20. LIMITATION OF ABSTRACT UL	

High-Frequency Planar Power Transformer
for Switching Power Supplies

Final Progress Report

Hung David Yang
Pervez A. Dalal
Ming Y. Ng
Tzung-Ta Kao
C.Q. Lee

January 25, 1996

U.S. Army Research Office
Grant no. DAAH04-95-1-0409

University of Illinois at Chicago

APPROVED FOR PUBLIC RELEASE;
DISTRIBUTION UNLIMITED.

THE VIEWS, OPIONS, AND/OR FINDINGS CONTAINED IN THIS REPORT ARE THOSE
OF THE AUTHORS AND SHOULD NOT BE CONTRUED AS AN OFFICIAL
DEPARTMENT OF THE ARMY POSITION, POLICY, OR DECISION, UNLESS SO
DESIGNATED BY OTHER DOCUMENTATIONS

TABLE OF CONTENTS

SECTION	PAGE
I. Problem Statement and objectives	5
II. Isolated Transmission-Line Transformer Analysis	6
III. Integrated Transmission-Line Transformer Design	12
III.1. Parallel Striplines Analysis	12
III.2. High-Frequency Transformer Prototype Design	13
III.3. Low-Frequency Transformer Prototype Design	30
IV. Conclusions	35
V. Bibliography	36

LIST OF TABLES

TABLE	PAGE
I. Design Data for Prototype Transformer A, B, C, and D	17
II. design Data for Prototype Transformer E	31

LIST OF FIGURES

FIGURE	PAGE
1. A Transmission Line Section	6
2. Isolated Interconnected Transmission Lines	7
3. Two Equivalent Transmission Lines	8
4. Cascaded Isolated Transmission-Line Transformer	9
5. Transformer with Three Transmission-Line Sections	10
6. Δf versus Z_{c2} for $Z_L = 1\Omega$ and $V_{ft} = 0.2$	11
7. The Cross-Section of Parallel Striplines and the Microstrip Equivalence ...	12
8. Prototype Transformer B Layout	14
9. Prototype Transformer C Layout	15
10. Prototype Transformer D Layout	16
11. Transformer B on a Test Fixture	19
12. Transformer C on a Test Fixture	20
13. Transformer D on a Test Fixture	21
14. $\text{Re}\{Z_{in} / Z_L\}$ of Transformer Prototype A	22
15. $\text{Im}\{Z_{in} / Z_L\}$ of Transformer Prototype A	23
16. $\text{Re}\{Z_{in} / Z_L\}$ of Transformer Prototype B	24
17. $\text{Im}\{Z_{in} / Z_L\}$ of Transformer Prototype B	25
18. $\text{Re}\{Z_{in} / Z_L\}$ of Transformer Prototype C	26
19. $\text{Im}\{Z_{in} / Z_L\}$ of Transformer Prototype C	27
20. $\text{Re}\{Z_{in} / Z_L\}$ of Transformer Prototype D	28
21. $\text{Im}\{Z_{in} / Z_L\}$ of Transformer Prototype D	29
22. The Top View of the Prototype Transformer E.....	32
23. The Bottom View of the Prototype Transformer E	33
24. Smith Chart Plot of the Input Impedance of a Step Down (1:4) Transformer E with a 50Ω load	34

I. Problem Statement and Objectives

In the past decade, there had been significant progress in the size reduction of digital integrated circuits (ICs). The miniaturization of ICs has not been matched by a similar reduction in the size of their power supplies. Furthermore, in most electronic equipment, integrated circuits require a high density of busses to distribute power at low supply voltage. DC/DC converters with switching frequency beyond MHz are the components of the future [1-2]. Although High-frequency operation has always associated with smaller energy storage components, conventional power transformer is resisting such a trend due to the increasing losses and parasitic effects associated with higher frequencies [3-4]. Skin and proximity effects dominate copper loss, and domain wall resonance phenomena raise hysteresis loss. Parasitic inductance becomes a significant part of total circuit inductance. Essentially, the power transformer has to be redesigned for the required high-frequency operation without sacrificing the conventional transformer functions of electrical isolation and high turn ratios, or reducing its power-handling capabilities [5].

Mega-Hertz operation reduces the magnetic components required in the power supply to the point where thick and thin film fabrication techniques can be applied to the conductor windings [6]. As the switching frequencies increase and the weight and volume constraints become more stringent, the traditional hybrid approach with discrete components and wired interconnection becomes very limited. Integrated solid-state and reactive components including transformers are the desirable components of the future [7-8].

In the past, numerous work has been done on the subject of high-frequency transformers. The research has been focused on two main subjects: (1) More accurate analytic and numerical models for transformers for better understanding of the mechanism and better design, (2) The improvement of transformer structures for better performance [5-10]. The minimization of conductor loss, hysteresis loss and eddy-current loss, the reduction of leakage inductance, the increase of the magnetizing inductance, the reduction of size and weight, and the increase in power-handling capability are the issues being addressed. Up to now, transformers with acceptable performance can be operated up to only 10 MHz [10]. The fundamental limitation of present transformer structure is the necessity of utilizing ferrite cores where the material properties are undesirable for higher frequencies.

An ultimate power transformer for high-frequency operation should have the features of compactness in size, light weight, no core, planar integration, electrical isolation, high efficiency, and high power handling capability. This project deals with the design and the prototype development of a new type of power transformer: **Transmission-line transformer**. The transformer is consisted of the **cascade of printed interconnected striplines in a planar structure**, where energy storage and transfer is through **electromagnetic waves**. The analysis and the design of such a structure are based on classical electromagnetic-wave theory in a guided wave structure. Five transformer prototypes are developed. Prototype A is for a 50 MHz coaxial-line transformer, Prototypes B, C, and D are for a hundred MHz printed strip-line transformers, and Prototype E is for an 8 MHz printed strip-line transformer. The developed transmission line transformers are particularly suitable for high frequency operation and will have significant impact on the future power electronics industry.

II. Isolated Transmission-Line Transformer Analysis

Application of transmission line principles to the design of high frequency resonant L and C in power converter has been proposed recently [11-12]. It has been shown that by employing large ϵ and μ to reduce the transmission line wavelength, it is possible to design transmission line resonator with reasonable dimension (15 cm in length) at frequency 10 MHz. Transmission-line transformer (TLT) had been used in impedance matching in antenna networks in radio or microwave frequency [13]. The idea of employing transmission line transformers in switching power is to provide voltage step-up or step-down in a prescribed manner at a single frequency[14]. At the design frequency, the transmission line transformer is made of cascade of quarter-wave transmission lines. The basic theory of a transmission-line transformer is described in this section.

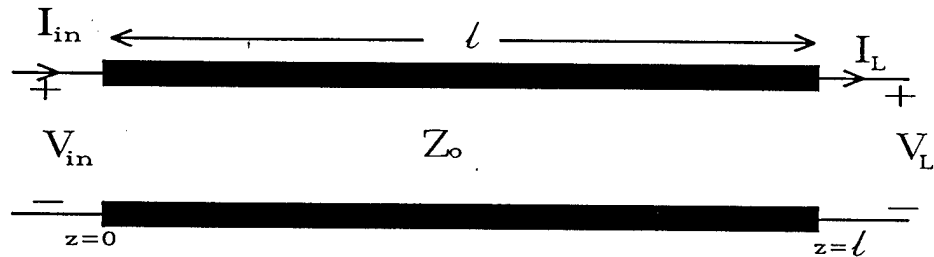


Figure 1. A transmission line section

Figure 1 shows a section of transmission line of length l . The input current and voltage are related to the output current and voltage through an ABCD matrix as [15]

$$\begin{bmatrix} V_{in} \\ I_{in} \end{bmatrix} = \begin{bmatrix} A & B \\ C & D \end{bmatrix} \begin{bmatrix} V_L \\ I_L \end{bmatrix} \quad (1)$$

with

$$\begin{bmatrix} A & B \\ C & D \end{bmatrix} = \begin{bmatrix} \cos(\ell\beta) & jZ_0 \sin(\ell\beta) \\ j\frac{\sin(\ell\beta)}{Z_0} & \cos(\ell\beta) \end{bmatrix} \quad (2)$$

β and Z_0 are the propagation constant and characteristic impedance of the transmission line, and the line is assumed lossless. For a quarter-wave transformer $\ell\beta = \pi/2$, the input and output impedance are related through the formula $Z_{in} = Z_0^2 / Z_L$. In a conventional power transformer, the input and output impedance ratio is a constant independent of the load. In order to simulate such a situation in a transmission-line transformer, we need to use the cascade of two quarter-wave transformers. If the line impedances are Z_{01} and Z_{02} , respectively for the first and the second quarter-wave lines, the impedance ratio will be Z_{01}^2 / Z_{02}^2 . We will come back to this

later. One of the important features of a power transformer is the DC isolation. It is seen that conventional quarter-wave transformer is DC short circuited. In order to overcome this difficulty, isolated interconnected transmission lines have been proposed [16]. The geometry of isolated interconnected transmission lines are shown in Figure 2.



Figure 2. Isolated interconnected transmission lines.

In order to derive the general circuit parameters, a balance transmission line assumption is made i.e. the current in one conductor of a transmission line is equal in magnitude but opposite in direction to each other. Thus, with a_1 and b_1 nodes connected, the current entering a_2 is forced to be identical to the current emerging from b_1 . Also, the currents at the nodes c_1 and d_2 are the same. If we assume the electrical lengths of the two transmission lines are the same. In other words,

$$\ell\beta = \ell_1\beta_1 = \ell_2\beta_2 \quad (3)$$

If the terminal nodes are defined according to Figure 2, the ABCD matrix of isolated transmission lines can be found as

$$\begin{bmatrix} A & B \\ C & D \end{bmatrix} = \begin{bmatrix} \cos(\ell\beta) & j(Z_{01} + Z_{02}) \sin(\ell\beta) \\ j \frac{\sin(\ell\beta)}{Z_{01} + Z_{02}} & \cos(\ell\beta) \end{bmatrix} \quad (4)$$

It is noted that the isolated transmission lines in Figure 2 result a chain matrix ABCD identical to that for a single transmission line section, if we let $Z_0 = Z_{01} + Z_{02}$. The interconnection of lines in Figure 2 results in DC isolation and the characteristic impedance that is the sum of the impedances of the two lines. This equivalence is shown in Figure 3.

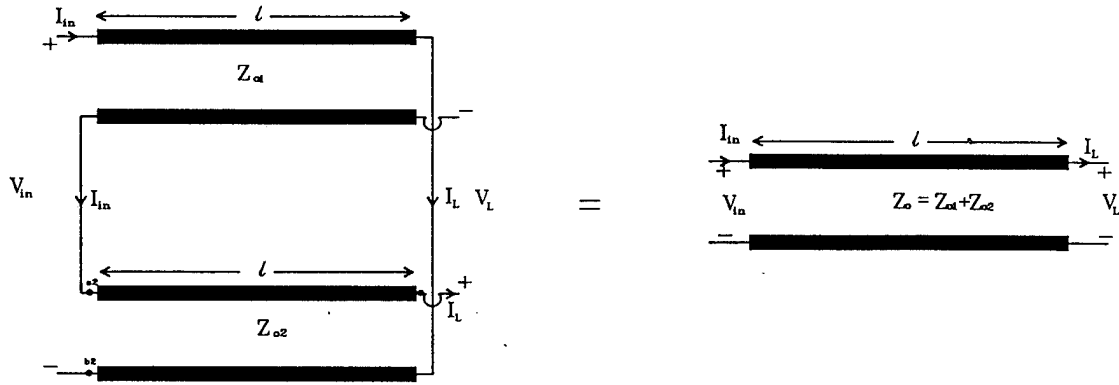


Figure 3. Two equivalent transmission-lines.

As was mentioned previously, conventional transformer response can not be obtained from a single quarter-wave transmission line section (isolated or not). However, the cascade of two isolated quarter-wave transmission lines shown in Figure 4 can result conventional transformer response. This analysis is described in the following. For the first section of the cascade, we have

$$\begin{bmatrix} V_{in} \\ I_{in} \end{bmatrix} = \begin{bmatrix} A_1 & B_1 \\ C_1 & D_1 \end{bmatrix} \begin{bmatrix} V_{L1} \\ I_{L1} \end{bmatrix}, \quad (5)$$

while for the second section of the cascade, we have

$$\begin{bmatrix} V_{L1} \\ I_{L2} \end{bmatrix} = \begin{bmatrix} A_2 & B_2 \\ C_2 & D_2 \end{bmatrix} \begin{bmatrix} V_L \\ I_L \end{bmatrix}. \quad (6)$$

For the overall circuit, we have

$$\begin{bmatrix} V_{in} \\ I_{in} \end{bmatrix} = \begin{bmatrix} A & B \\ C & D \end{bmatrix} \begin{bmatrix} V_L \\ I_L \end{bmatrix}, \quad (7)$$

where

$$\begin{bmatrix} A & B \\ C & D \end{bmatrix} = \begin{bmatrix} A_1A_2 + B_1C_2 & A_1B_2 + B_1D_2 \\ C_1A_2 + D_1C_2 & C_1B_2 + D_1D_2 \end{bmatrix}. \quad (8)$$

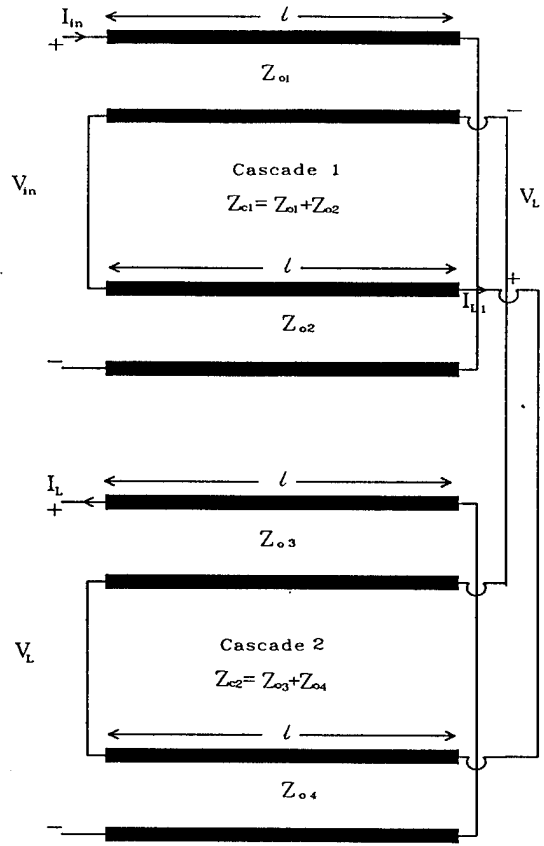


Figure 4. Cascaded isolated transmission-line transformer

If we define $Z_{c1} = Z_{o1} + Z_{o2}$ and $Z_{c2} = Z_{o3} + Z_{o4}$, and use the formula of ABCD matrix for a transmission line section, we have

$$\begin{bmatrix} A & B \\ C & D \end{bmatrix} = \begin{bmatrix} \cos^2(\ell\beta) - \sin^2(\ell\beta) \frac{Z_{c1}}{Z_{c2}} & j \sin(\ell\beta) \cos(\ell\beta) (Z_{c1} + Z_{c2}) \\ j \sin(\ell\beta) \cos(\ell\beta) \left(\frac{1}{Z_{c1}} + \frac{1}{Z_{c2}} \right) & \cos^2(\ell\beta) - \sin^2(\ell\beta) \frac{Z_{c2}}{Z_{c1}} \end{bmatrix} \quad (9)$$

From Equation (9) we can determine the relation between the input Z_{in} and output (load) Z_L impedance of the transformer.

$$Z_{in} = \frac{AZ_L + B}{CZ_L + D} \quad (10)$$

It is noted that at a quarter-wave length $\ell\beta = \pi/2$, $B = C = 0$ and

$$\frac{Z_{in}}{Z_L} = \left(\frac{Z_{c1}}{Z_{c2}} \right)^2 \quad (11)$$

The transformer voltage ratio is noted as $N = Z_{c1} / Z_{c2}$. The observation in Equation (11) is rather interesting. It shows that the transformer ratio is determined only by the transmission line impedance.

The transformer circuit topology in Figure 4 can be simplified by the fact that the isolated transmission lines are equivalent to a transmission line as shown in Figure 3. If the first section in Figure 4 is replaced by a single-section transmission line with an equivalent impedance, the characteristics of the transformer remain unchanged, but the total number of transmission lines reduced from four to three as shown in Figure 5. This improvement of reducing the total physical length of a transformer by 25% is rather significant. It is noted that the resulting transformer is DC isolated. The resemblance of the transmission line transformer and the conventional transformer is observed when the total electrical length is half wavelength. Since a transmission line has periodic characteristics, same response could be observed at the line length that is integer multiple of half wavelength.

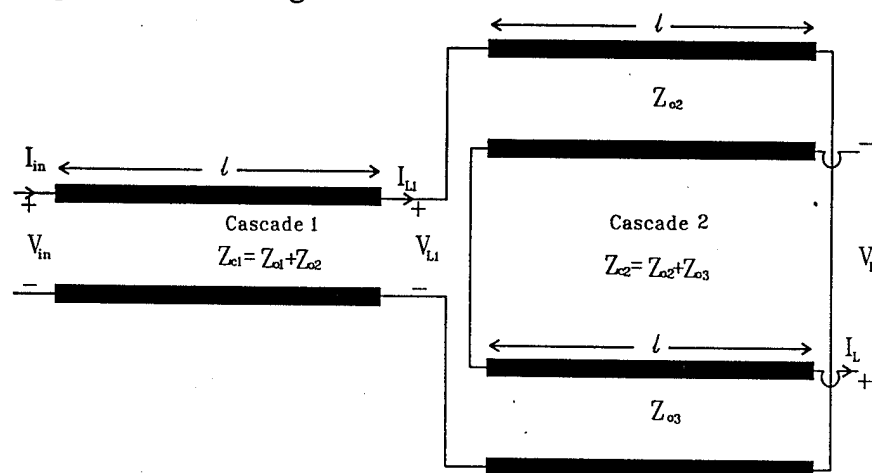


Figure 5. Transformer with three transmission-line sections.

The proposed transmission-line transformer resembles to a conventional transformer at the quarter-wave frequency f_0 . It is noted from Equations (9) and (10) that the voltage or impedance ratio is frequency and load dependent, and any deviation of frequency from f_0 causes degradation of the transformer performance. For practical purpose, it is of interest to know the frequency response of the transformer ratio and have proper design to extend the useful frequencies. For the convenience of analysis, we define the following parameters: fractional voltage tolerance V_{ft} as the deviation of voltage ratio due to frequency shift normalized by the N , the desired voltage ratio, fractional bandwidth $\Delta f = 2(f_0 - f_1) / f_0$ with

f_1 the lower band frequency. If the frequency f_1 is close to f_0 so that $\cos^2(\ell\beta)$ can be ignored, the voltage ratio can be approximated as

$$\frac{V_{in}}{V_L} = -N + j \frac{Z_{c2}}{Z_L} \frac{N+1}{\tan(\ell\beta)} \quad (12)$$

Also,

$$V_{ft} = \frac{Z_{c2}}{Z_L} \frac{N+1}{N \tan(\ell\beta)} \quad (13)$$

Δf is found as

$$\Delta f = 2 - \frac{4}{\pi} \frac{Z_{c2}}{Z_L} \frac{N+1}{N V_{ft}} \quad (14)$$

Equation (14) provides an important design formula. If $V_{ft} = 0.2$ is the maximum value one can tolerate, the transmission line impedance Z_{c2} can be properly chosen to achieve desirable bandwidth Δf . An example of this design information is shown in Figure 6. For three different N , Δf is plotted against Z_{c2} for $Z_L = 1\Omega$ and $V_{ft} = 0.2$. It is interesting to see that the small Z_{c2} is, the larger the bandwidth Δf would be.

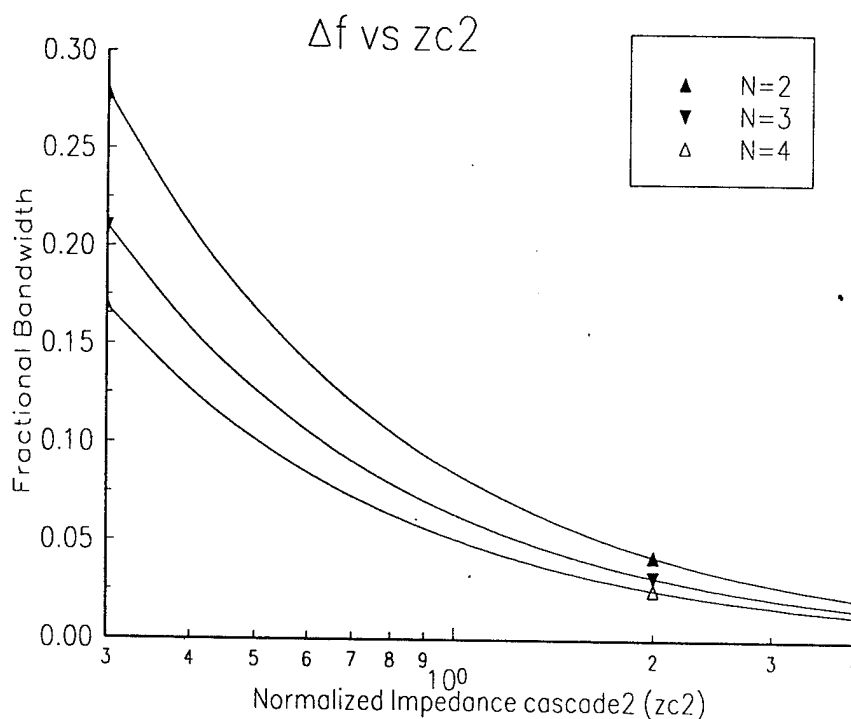


Figure 6. Δf versus Z_{c2} for $Z_L = 1\Omega$ and $V_{ft} = 0.2$.

III. Integrated Transmission-Line Transformers Design

In the previous section, we described the fundamental theory of how a transmission -line transformer work without specifying the geometry and shape of the structure. The drive to achieve **low-profile, higher-density** switching power supplies has led to the development of transformers using multi-layer printed circuit boards with etched conductors that functions as the transformer windings. The turns at each layer are connected in series or in parallel through via holes. Due to the small tolerances of printed circuit board manufacturing, the winding geometry is easily reproducible. Thin copper layers reduce skin-effect losses. The flat configuration provides a relatively large surface area for the transfer of dissipated heat to the environment. The transformer can be an integrated part of a circuit board with other components. In this project, the design and prototype development of transformer use integrated guided wave structures (microstrip lines) as the transmission lines.

III.1 Parallel striplines analysis

From the theory described in the previous section, it is seen that the transformer properties depend on the propagation constants and the characteristic impedances of the transmission lines. These characteristics are functions of the geometrical parameters. The selection of the configuration is essential to the transformer performance. In this project, printed parallel striplines and their equivalent structure shown in Fig. 7 are selected as the transmission line structure for transformers. Parallel striplines are consisted of two thin metallic films each bonded to the surface of a slab. The material properties, its thickness, and the width of the metallic films determine the propagation constant and characteristic impedance of a stripline.

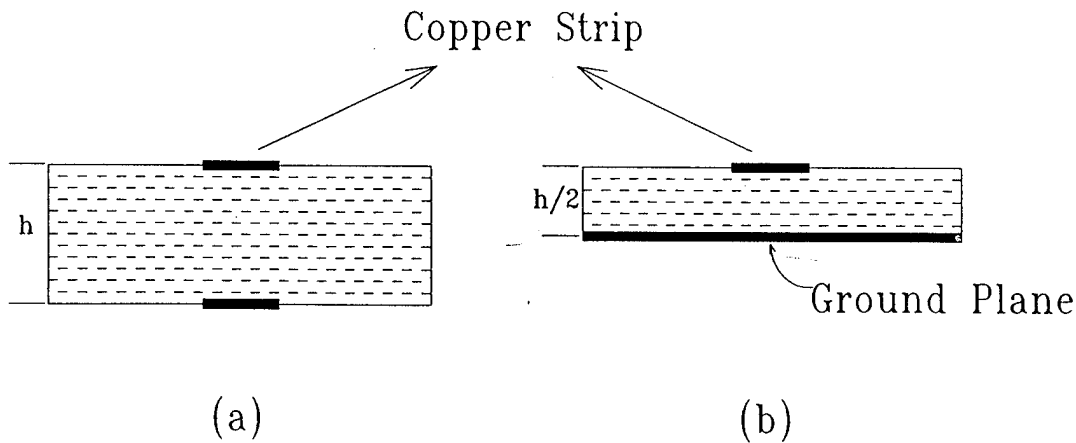


Figure 7. The cross-section of parallel striplines and the microstrip equivalence.

It is noted that for the fundamental mode, the electric field lines emanate from one strip and terminate on the other. Due to the symmetry, it is possible to place a perfect conductor at the center of the slab without changing the field distribution of the structure. The resulting structure is two isolated microstrip transmission line shared a common ground. Without losing

the generality, we need to consider only half of the structure, but bear in mind that there is actually twice of power flow in the structure. The design of printed stripline transformers requires the information of the propagation constants (wave number) and the characteristic impedances of the striplines. The propagation constants are used to determine the length of each stripline. The characteristic impedances are used to determine the transformer voltage ratio (the relation is give in Equation 11) or the impedance matching in the input port. The solutions of an electromagnetic boundary value problem shown in Figure 8 are needed to obtain these two parameters. It is a good assumption that the geometry is infinite large and homogeneous in the planar directions since most of the energy (fields) is confined within the region near the stripline. Also, since the transmission line characteristics are what we are looking for, the stripline by itself is considered infinite long. The boundary value problem is a two dimensional problem (cross section), where various numerical approaches are possible. Among them, spectral domain integral equation method is more appealing in this problem. The details of this approach are discussed in Reference [17]. In this project, empirical formulas shown in literature [18] are used to compute the phase constant and the line impedance. For the completeness, these formulas are given in the following equations. If the width of the strip is w , slab thickness h , dielectric constant ϵ_r , free space wave number k_0 , the phase constant β , and the characteristic impedance Z_0 , we have

$$\beta = k_0 \sqrt{\epsilon_{eff}} \quad , \quad (15)$$

$$\epsilon_{eff} = \frac{\epsilon_r + 1}{2} + \frac{\epsilon_r - 1}{2} \frac{1}{\sqrt{1 + (5h/w)^2}} \quad , \quad (16)$$

$$Z_0 = \frac{240}{\sqrt{2(\epsilon_r + 1)}} \left[\ln\left(\frac{4h}{w}\right) + \frac{(w/h)^2}{8} - \frac{\epsilon_r - 1}{2(\epsilon_r + 1)} \left\{ \ln(\pi/2) + \frac{\ln(4/\pi)}{\epsilon_r} \right\} \right] \quad , \quad (17)$$

for $w/h \leq 0.85$, and

$$Z_0 = \frac{120}{\sqrt{\epsilon_r}} \left[\frac{w}{h} + \frac{\ln 4}{\pi} + \frac{\epsilon_r + 1}{2\pi\epsilon_r} \left\{ \ln\left(\frac{\pi e}{2}\right) + \ln\left(\frac{w}{h} + 0.94\right) \right\} + \frac{(\epsilon_r - 1) \cdot \ln(e\pi^2/16)}{2\pi\epsilon_r^2} \right]^{-1} \quad , \quad (18)$$

for $w/h \geq 0.85$.

III.2 High-Frequency Transformer Prototype Design

In this project several transmission-transformer prototypes are developed utilizing printed striplines. First we consider strip-line transformers built on a Teflon-fiberglass with dielectric constant $\epsilon_r = 4.2$ and thickness 0.54 mm. The transformers are formed by photo-etching both

sides of the 4 oz. copper-clad dielectric slab. The remaining unetched pattern on top and bottom forms a single transmission line section.

A major design concern is the compactness in size. Therefore, the transformer layouts are designed to minimize the area of the dielectric plate without compromising the transformer performance. There are essentially two ways to accomplish this objective (i) utilizing the geometrical shapes of the strip-lines, (ii) using multi-layer structures. In this project, we explore both possibilities. In stead of making strip lines straight, the conductors are patterned into layouts that occupy much greater length in a given area as compared to straight-line conductors. Three types of circuit layout are made and shown in Figures 8-10, respectively, for transformer B, C, and D. Transformer A is coaxial-cable transformer. The resulting transformer circuitries are meander-line like with many bends and turns. In order to minimize the discontinuity effects, round corners with mean radius equal to 1 to 1.5 times the strip width are used. With the frequency of interest, the discontinuity effects for those round corners are negligible. Also, the round corners are easier and more accurate in fabrication due to the isotropic nature of the developer and etchant.

The multi-layer approach in the design can further reduce the overall transformer size. For the three line transformer shown in Figure 5, the two transmission line sections are built on different circuit board and with a spacing layer in between. The multi-layer integration is complicate by the interconnection through the three-layer structure.

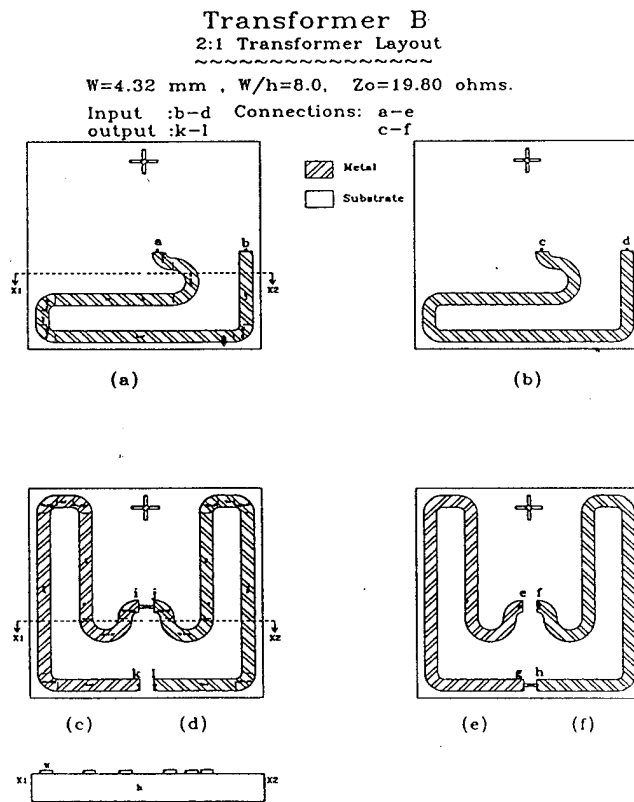


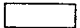

FIGURE 8. (a), (b) Top and Bottom views Layer 1. (c), (e) Bottom and top views Layer 2. (d), (e) Bottom and top views Layer 3. (g) Crosssectional view.

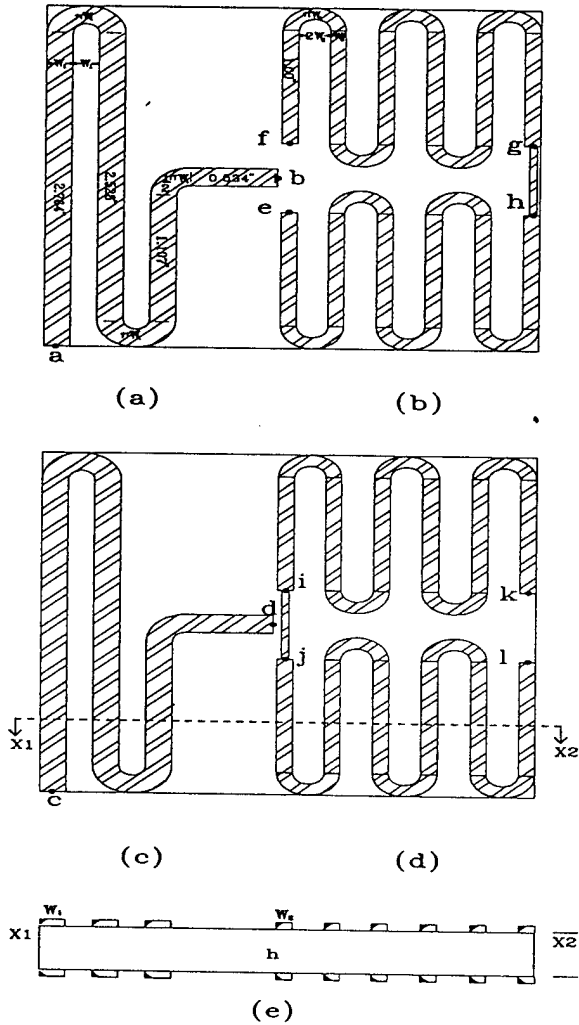
Transformer C

3:1 Transformer Layout

~~~~~

$W = 4.00\text{mm}$   
 $W = 2.50\text{mm}$   
 $W_1 = 7.40$   
 $h = 2.50$   
 $W_2 = 4.60$   
 $h = 2.50$   
 $Z_{o1} = 21.21 \text{ ohm}$   
 $Z_{o2} = 31.81 \text{ ohm}$   
 Input : a-c  
 output: k-l  
 Connections:  
 b-e  
 d-f

 Substrate  
 Metal



(a), (b) Top views  
 (c), (d) Bottom views  
 Layer 1 and 2.  
 (e) Crosssectional view.

FIGURE 9.


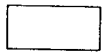
# Transformer D

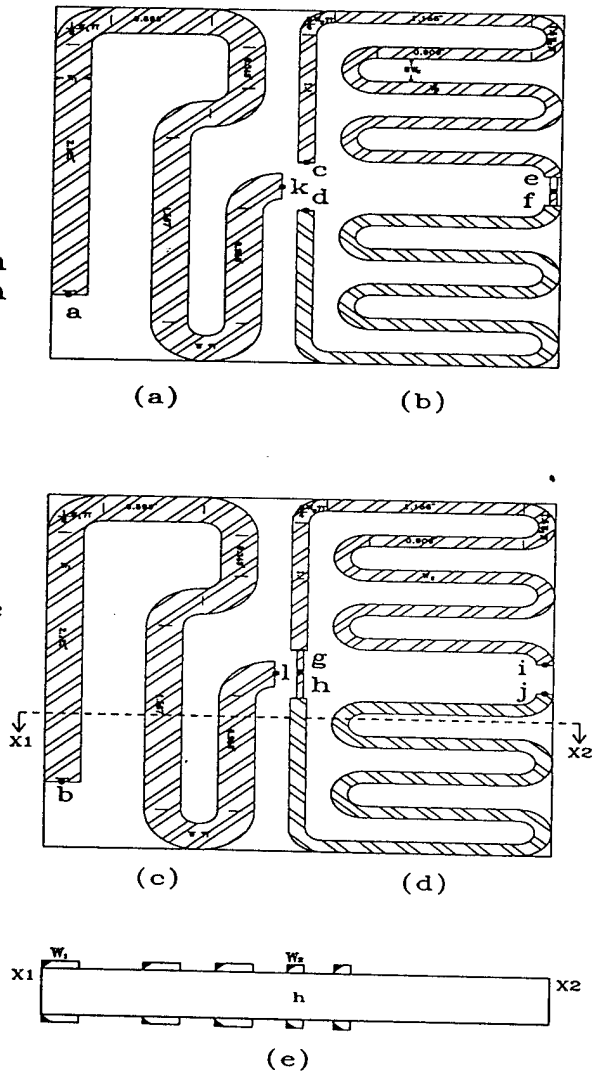
## 4:1 Transformer Layout

~~~~~

$W_1 = 5.51\text{mm}$
 $W_2 = 2.50\text{mm}$
 $\frac{W_1}{h} = 10.20$
 $\frac{W_2}{h} = 4.60$
 $Z_{o1} = 15.94 \text{ ohm}$
 $Z_{o2} = 31.81 \text{ ohm}$

Input :a-b
 output:i-j
 Connections:
 k-c
 l-d

 Metal
 Substrate



(a), (b) Top views
 (c), (d) Bottom views
 Layer 1 and 2.
 (e) Crosssectional view.

FIGURE 10.

The prototype transformer design data is shown in Table I for Transformer A, B, C, D. The stripline impedance and quarter-wave length are determined from the design formulas shown in Equations 15-18. Cable transmission line transformer (Transformer A) is also developed for comparison. The design data for coaxial lines are found from literature [19].

Table I Prototype Transformer Data				
Transformer	A	B	C	D
Type Cascade 1:1 TL Cascade 2:2 TL	Cable	Strip	Strip	Strip
Turn Ratio (Secondary/Primary)	1.47	2	3	4
$Z_{c1}(\Omega)$	76	19.8	21.2	15.9
$Z_{c2}=Z_{c1}+Z_{c2}$ (Ω)	48+68	19.8+19.8	31.8+31.8	31.8+31.8
$Z_L(\Omega)$	50	50	50	50
QuarterWave Frequency (MHz)*	50	105	115	110
Strip Width Cascade1 Cascade2 (cm)	----	0.432 0.432	0.400 0.250	0.510 0.250
Substrate Thickness(cm) ϵ_r	----	0.054 4.2	0.054 4.2	0.054 4.2
Size(cm ²)	----	2.5X3.6	2.5X3.8	2.5X3.8
Integration	----	3-Layer	2-Layer	2-Layer

The prototype transformers are fabricated with a standard photo-lithography and etching techniques. The procedures are described in the following. The pattern layouts are made in AutoCAD and stored on a magnetic tape. The magnetic tape data is fed into PG-generator (e-beam device), which exposes the sensitized chrome glasses accordingly. The exposed pieces of glasses are developed in developer 851 solution for approximately 60 seconds. The chromium is etched in chrome etchant for about 40-60 seconds. The chromium patterns on the glasses are used as photo mask. The PC-board approximately 3" X 3" I placed in a tray with enough acetone to cover the board. The tray is placed in ultra sonic bath at 40 degrees C for five minutes and rinse in DI water. In the lithographic process, the board is spin coated with positive photo resist at 4000 r.p.m. for 30 seconds and prebaked at 90 degrees C for 15 minutes. The mask is aligned with the board in mask aligner. perimeter alignment is used. The board is exposed to UV light ($22.4 \text{ mW} / \text{cm}^2$) for 10 seconds. Exposed board is developed in solution for 60 seconds and rinse in DI water and dry in air. In the etching process, the board is etched by placing it in ferric chloride solution (completely immersed) heated at about 50 degrees C in a plastic tray. The tray is agitated and board is flipped periodically to ensure uniform etching.

This process takes about 2 to 3 hours. The board is rinsed in tap water and immersed in acetone for few seconds to remove resist.

The transformer prototype B, C, and D (strip line transformers) are built, and the physical layouts on fixtures are shown in Figures 11-13, respectively for Transformer B, C, and D. The prototypes are tested using HP-3577A network analyzer with S-parameter set HP-35677A. The 50Ω load is used in all the cases in the frequency range of 100 KHz-200MHz. The prototype A was first constructed using coaxial cables to verify the theory before fabricating the strip-line transformers. The measured frequency response of the impedance ratio of the designed transformer prototypes are shown in Figures 14-21. In all the cases, the solid lines are the analytic prediction and the dotted lines are the measured results. It is seen from the measured data that at the designed frequencies, the transformer ratio pretty much agrees the designed values. In fact, it is observed that the agreement between theory and experiment is excellent for high frequencies. For lower frequencies, significant discrepancy is observed in all the transformers, especially for stripline transformers. This is due to the fact that for low frequencies, the strip lines no longer act like transmission lines and the current in the two lines are no longer opposite in directions. This phenomenon is more profound for higher voltage ratio transformers where the line characteristics are more distinct. In spite of the discrepancy, at the frequency range of interest, the transformer prototypes shows excellent performance.

For Transformer A, the design frequency is 50 MHz and impedance ratio is 0.463. It is seen from the measured results in Figures 14 and 15 that at 50 MHz, the real part of the impedance ratio has is about 0.46 and the imaginary part is close to zero as what was predicted. For Transformer B, the design frequency is 105 MHz and the impedance ratio is designed as 0.25. The measured results in Figures 16 and 17 show that the central frequency is 110 MHz where the impedance ratio is purely real and is about 0.24 close to what was predicted. It is interesting to observe that the real part of the impedance is insensitive to frequency and the imaginary part is almost linear to frequency near the design frequency. When the impedance ratio is not purely real, there is instantaneous power storage within the transformer. Transformers C and D shows similar frequency response as Transformer B. Very good results are found near the design frequency as shown in Figures 18-21. It is also very interesting to observe that near the design frequency, the impedance ratio can be expressed as

$$\frac{Z_{in}}{Z_L} \approx \left(\frac{Z_{c1}}{Z_{c2}} \right)^2 + j(f - f_0)\alpha, \quad (19)$$

where α is a complicate function of Z_L , Z_{c1} , and Z_{c2} . A small signal analysis of Equation (10) confirms this observation. It is interesting to see from Equation 19 that a series quarter-wave open-circuit tuning stub may be used to eliminate the imaginary part of the impedance ratio, and a broad band transformer may result. This issue should be an interesting subject for future research. The efficiency of the transformer prototypes developed for 100 MHz or above is expected to be very high due to the fact that estimated material and conductor losses are very small. The loss tangent for the Teflon-fiberglass is very low (in the order of 0.001). In this project, we are unable to make a power test, for the lack of proper hundred MHz power amplifier.

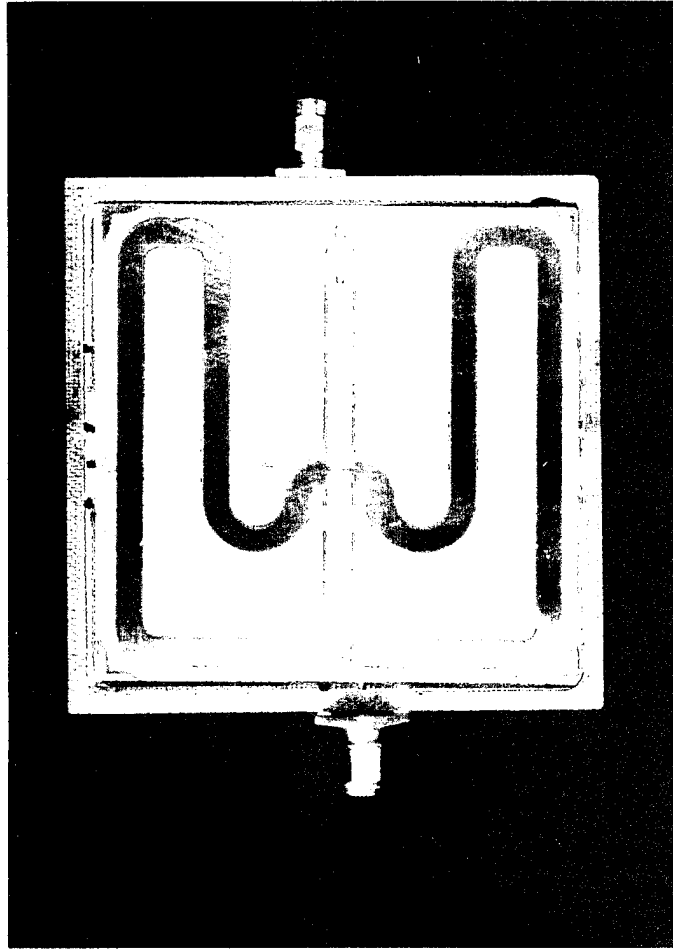


Figure 11 Transformer B. On Test Fixture

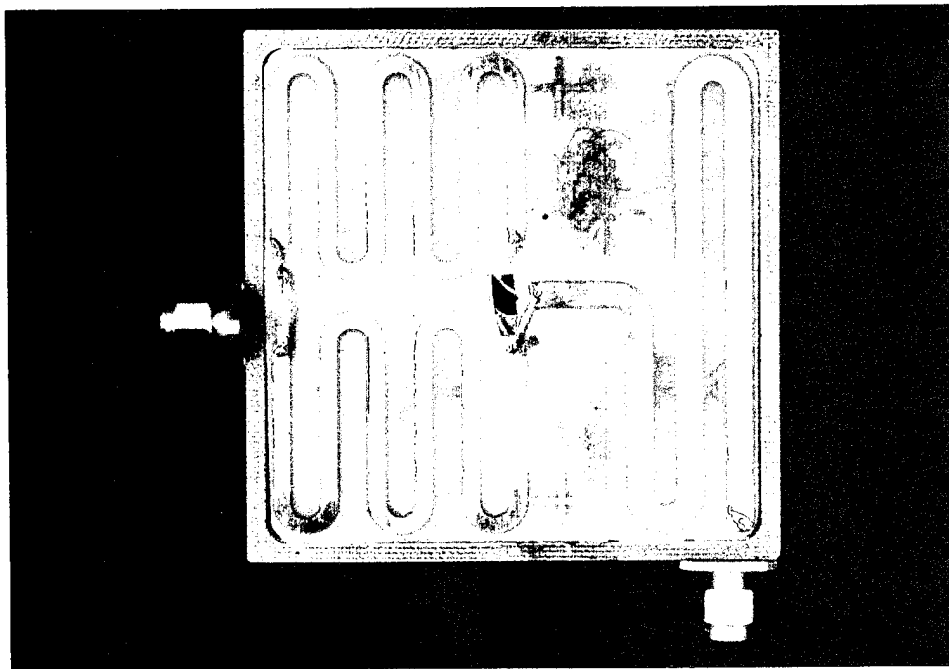


Figure 12 Transformer C. On Test Fixture

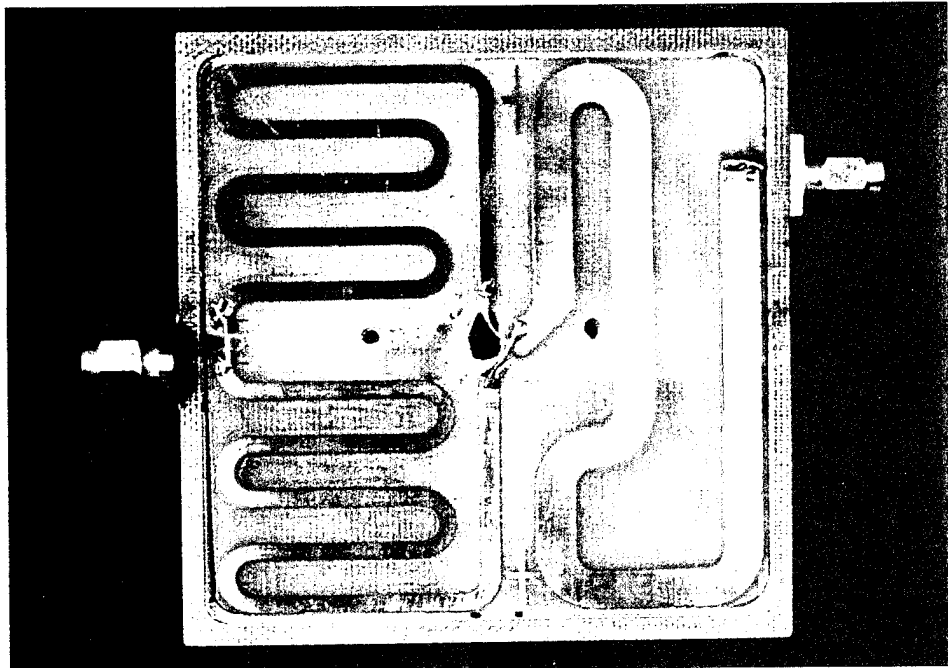


Figure 13. Transformer D. On Test Fixture

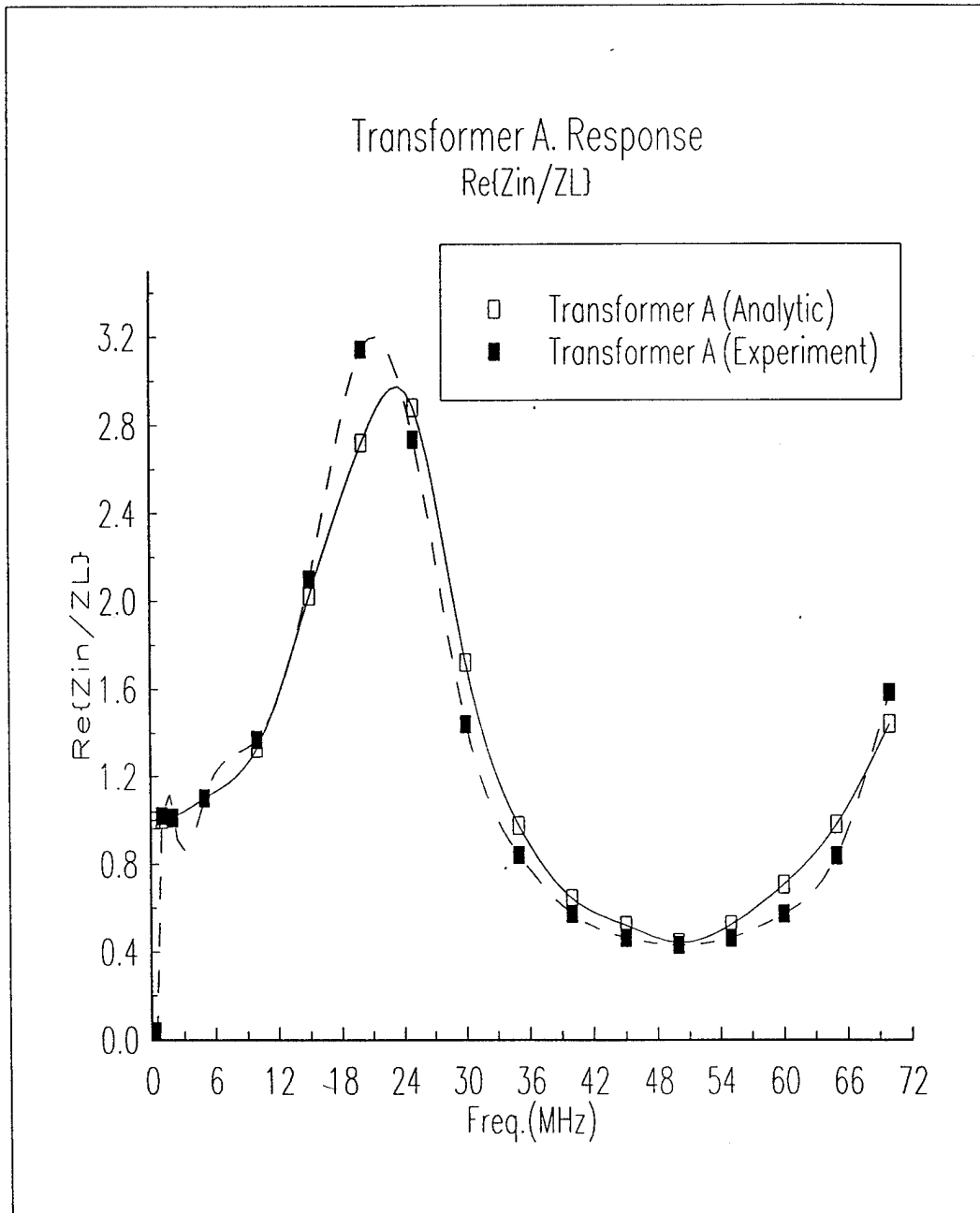


Figure 14 Transformer A. Re{Z_{in}/Z_L}

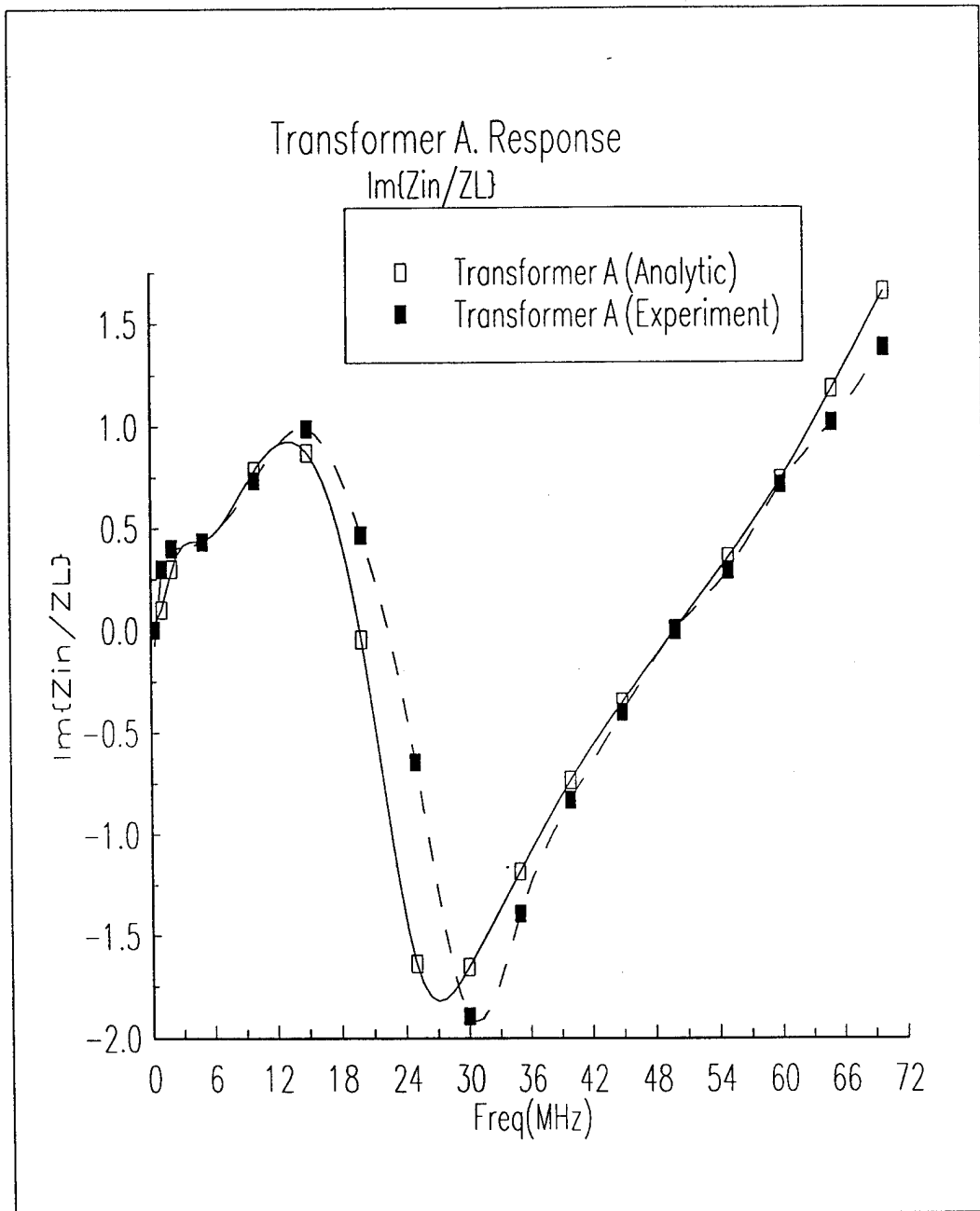


Figure 15 Transformer A. Im{Z_{in}/Z_L}

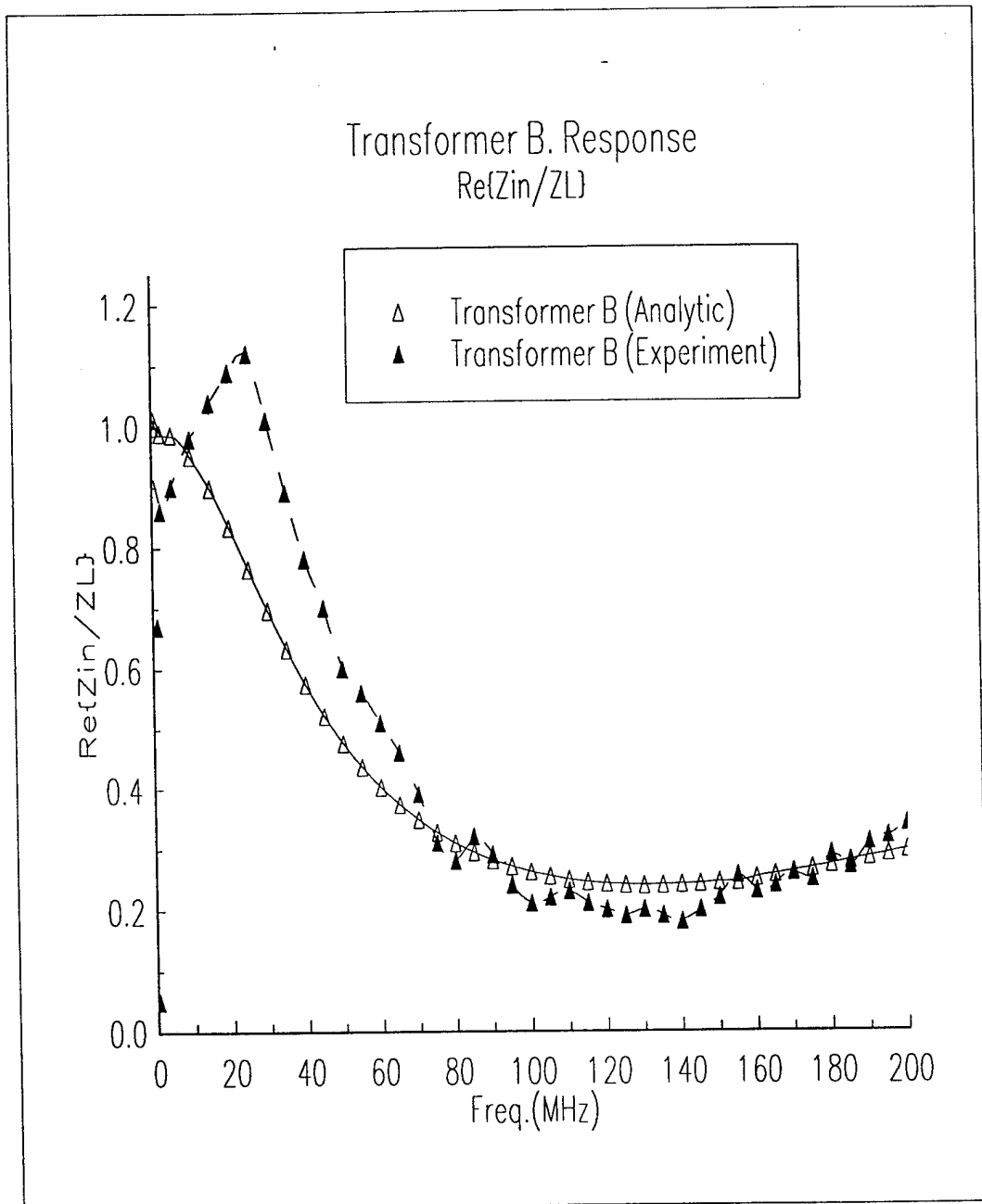


Figure 16 Transformer B. Re{Z_{in}/Z_L}

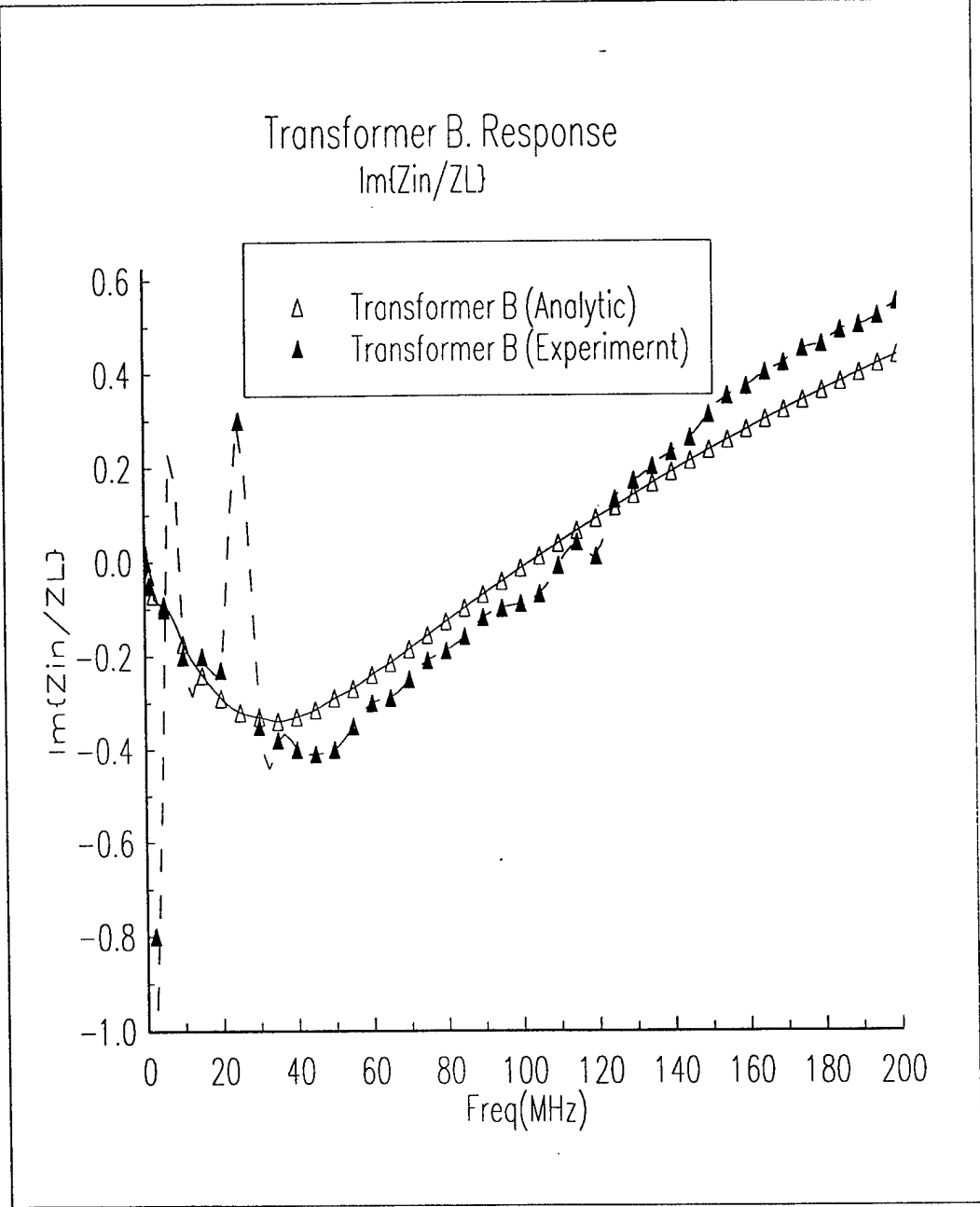


Figure 17 Transformer B. $\text{Im}\{Z_{in}/Z_L\}$

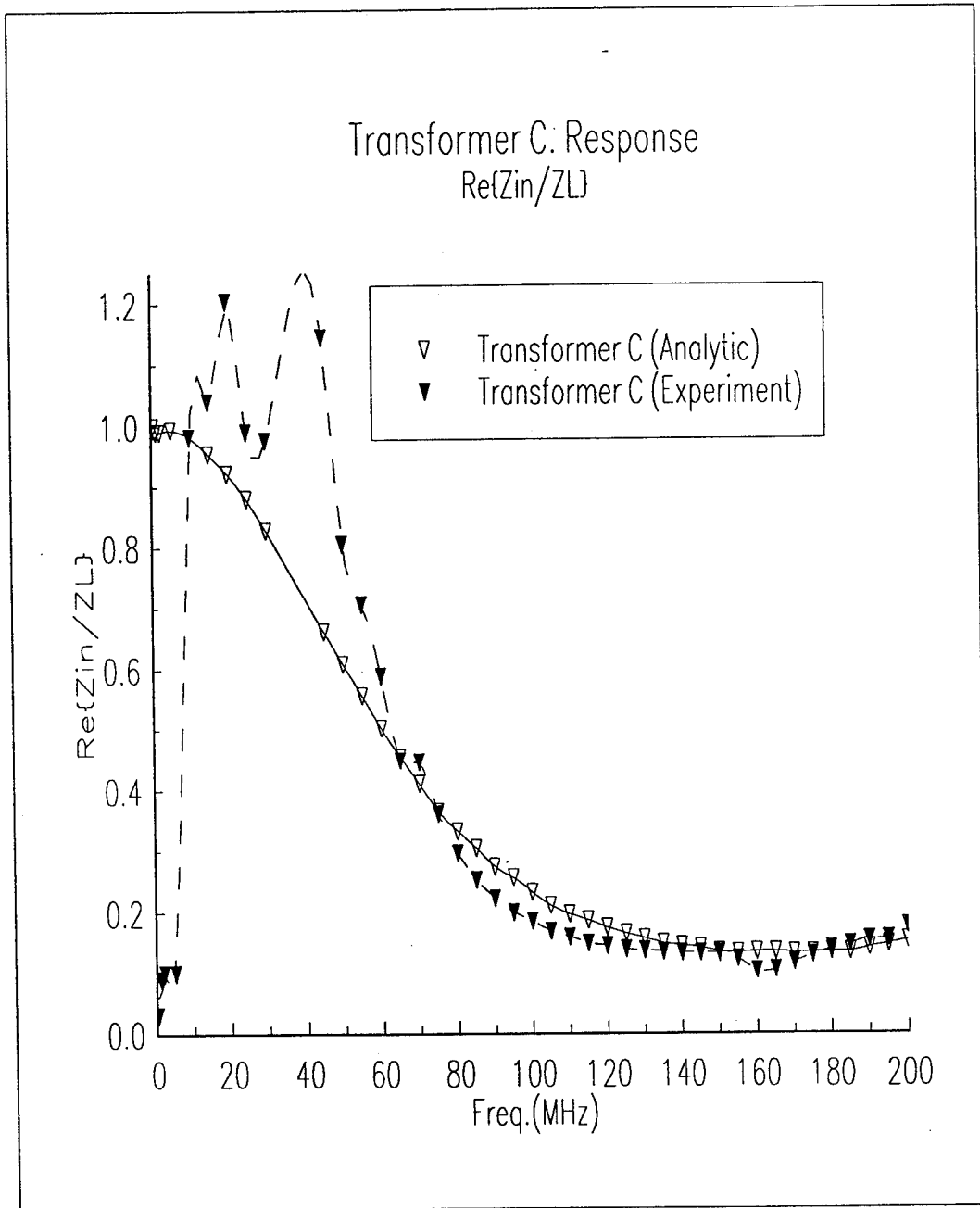


Figure 18

Transformer C. Re{Z_{in}/Z_L}

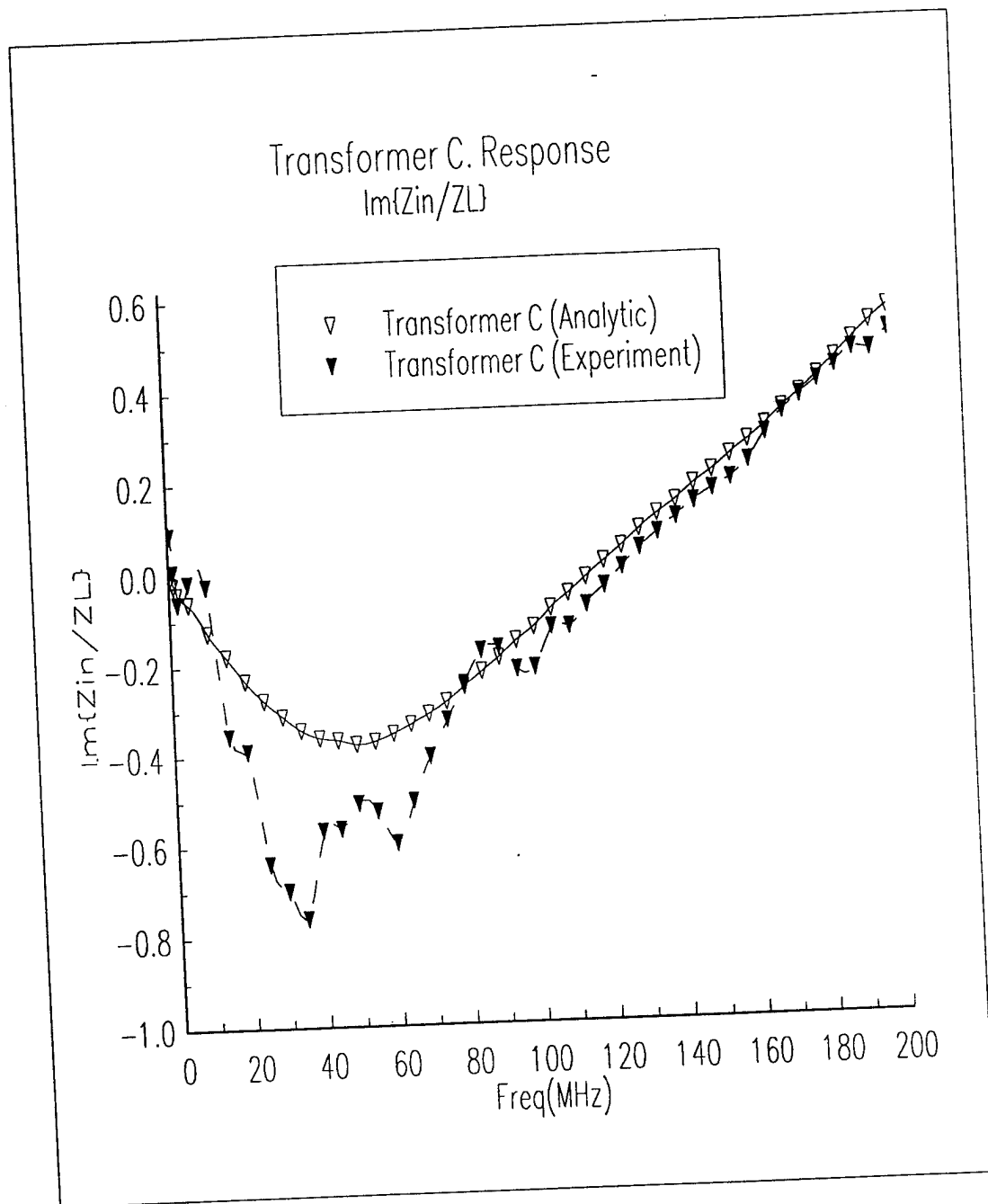


Figure 19 Transformer C. $\text{Im}\{Z_{in}/Z_L\}$

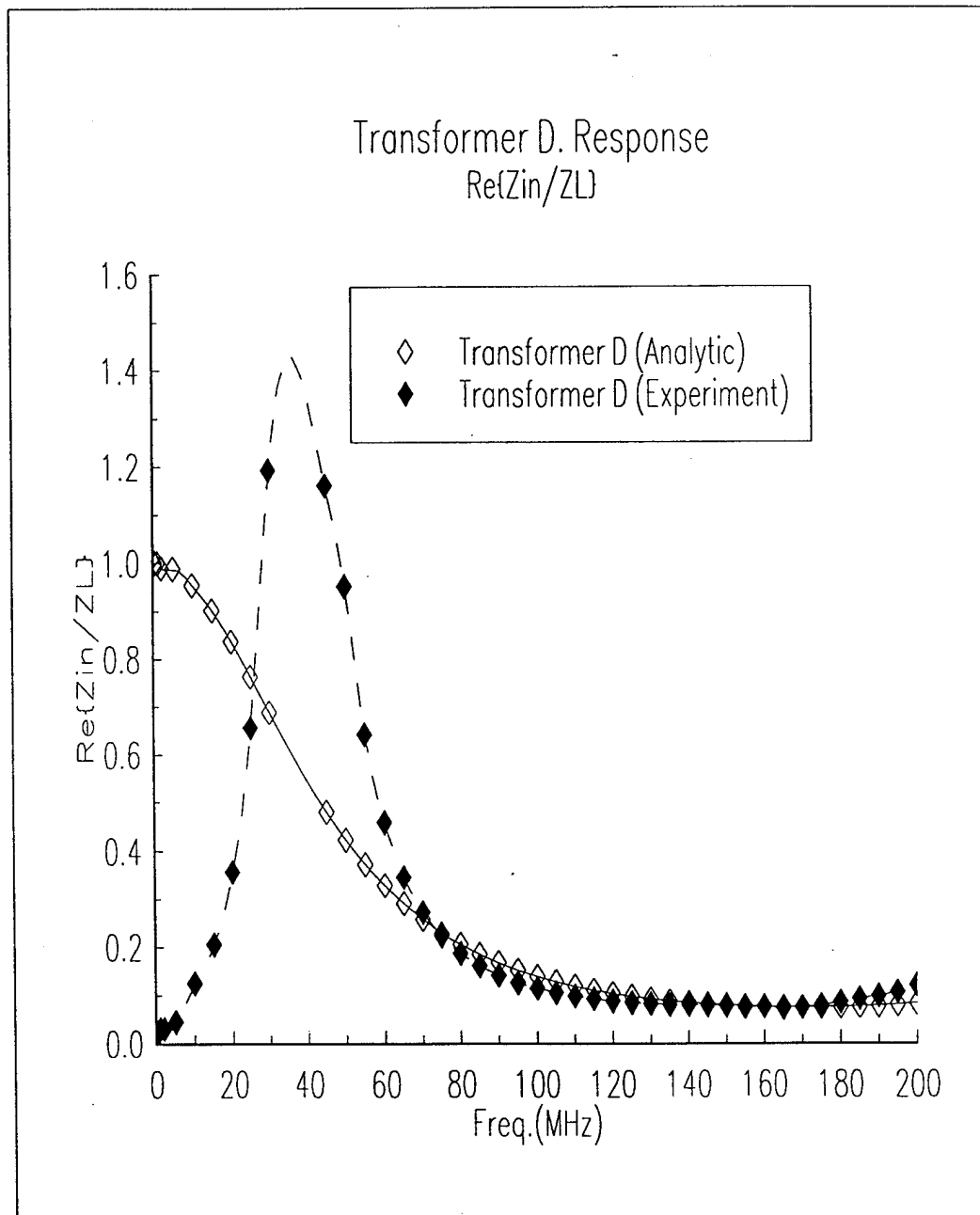


Figure 20 Transformer D. $\text{Re}\{Z_{in}/Z_L\}$

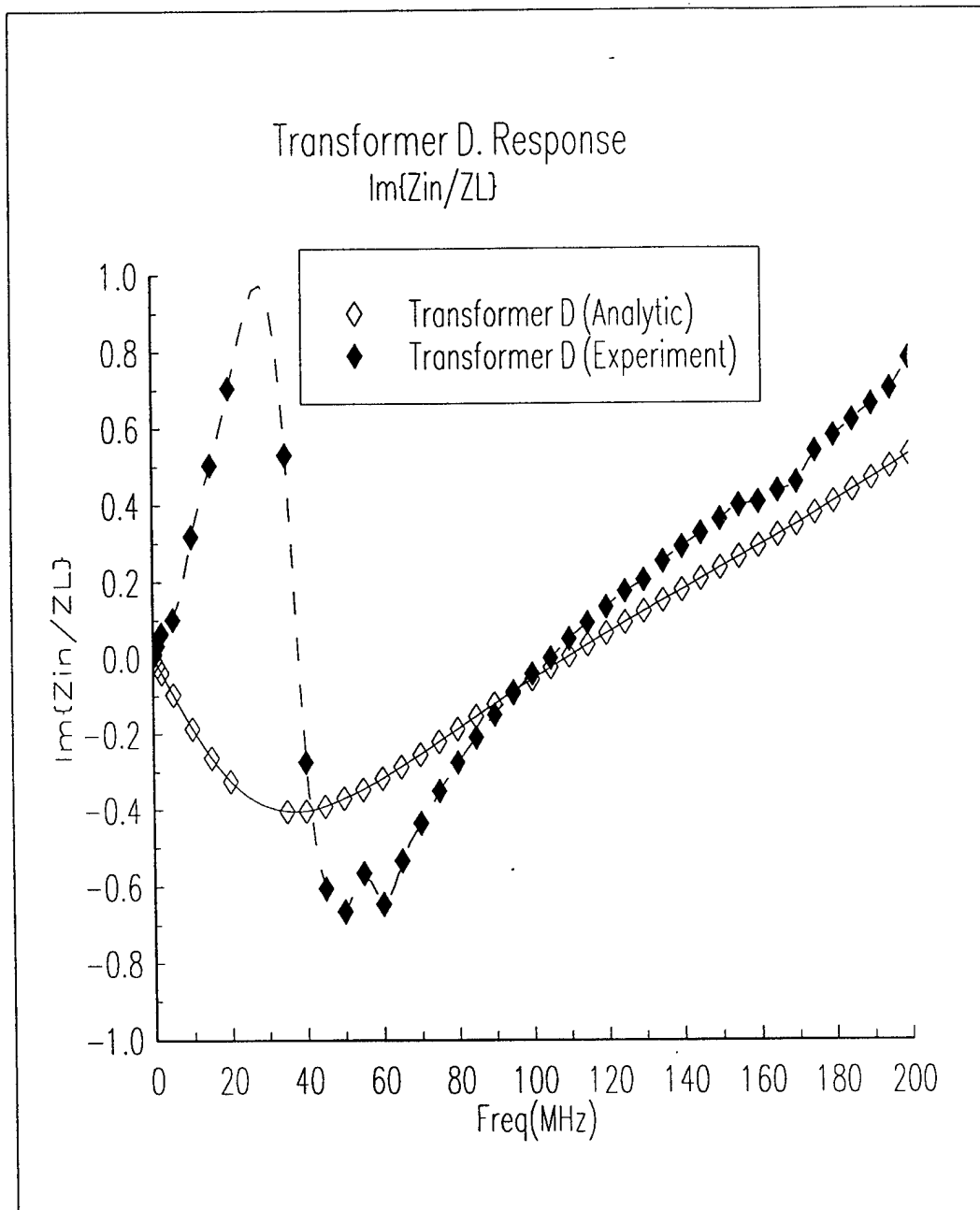


Figure 21 Transformer D. $\text{Im}\{Z_{in}/Z_L\}$

III.3 Low-Frequency Transformer Prototype Design

It is noted from Table I that the design frequency is around 100 MHz for stripline transformers (Transformer B, C, and D) and the slab area is about 9 cm square. The major problem of preventing the transformer for lower frequency operation while maintaining small component size is the wave length of the strip lines. For the Teflon-fiberglass $\epsilon_r = 4.2$, the quarter wave length at 10 MHz is over 3 meters! The required dielectric slab area is too large for any practical purpose. If the transmission line wave length is λ_g , we have

$$\lambda_g = \frac{c}{f} \frac{1}{\sqrt{\epsilon_{eff}}} \quad , \quad (20)$$

where ϵ_{eff} is given in Equation (16), c is the speed of light in free space, and f is frequency. It is seen that if we want to maintain small component size at low frequencies (around 10 MHz), λ_g must be reasonably small. This condition requires a large ϵ_{eff} or a large slab dielectric constant. Material with large dielectric constant (in the order of 1000) is not common. In this project, we use low-loss ceramics made of C-5800 lead Zirconate Titanate materials. The dielectric constant is around 1100. Transformer prototype E is built on such a material. The design frequency is at 8 MHz.

The ceramic plate has the surface area 3.1" x 3.1" and thickness 0.1 inch. A capacitance measurement confirms that the dielectric constant is indeed about 1100. The ceramic plate is not clad with metal layer. In order to build strip lines on such material, several methods were tried. First, we tried a thin metal-film deposition method. The problem for this approach is that the maximum metal-film thickness is only about 0.4 micron and at 8 MHz the skin depth is much larger than this thickness so that the ohmic loss is too large for practical purpose. Alternative approach which works quite well is to use silver paste over the ceramic plate. Thick silver layer is pasted over both side of the plate and the photo-lithography and etching techniques are used as before to produce the meandered transmission line pattern. The only deficiency for this approach is the roughness on the surface of the metal strips. For low MHz operation, this surface roughness would not affect the transformer performance much.

Transformer E design data is shown in Table II. The design is for impedance ratio 4:1 and the three striplines in Figure 6 are all identical. The strip line impedance is design to be 4.4 Ω and the line length of each stripline is about 40 cm (a quarter-wave length at 8 MHz). The quarter wave length frequency and the strip line impedance are measured by open-circuit and short-circuit tests. The measured results show the strip line impedance is about 4 Ω and the quarter frequency is found 8.3 MHz. Both parameters agree quite well with the design.

Since the length requirement for each strip is about 40 cm, the transformer can not be built on a single ceramic plate. Two plates with a spacing dielectric layer in between are used. Proper interconnection between lines are through the edge of the plates. The photographs of the physical transformer circuits are shown in Figures 22 and 23, respectively, from a top a bottom view.

Voltage Ratio	2
Z_{c1} (Ω)	4.4 (Theory) 4.0 (measured)
Z_{c2} (Ω)	8
Quarter-Wave Frequency (MHz)	8.0 (Designed) 8.3 (measured)
Strip Width (cm)	
Cascade 1	0.2
Cascade 2	0.2
Substrate Thickness (cm)	0.254
ϵ_r	1100
Surface Area (inch ²)	3.1 \times 3.1
Integration	3 Layers

From the design data shown in Table II, It is seen that by using Zirconate Titanate materials, we are able to bring down the transformer design frequency to low MHz while maintaining small overall size. However, in the process of making open-circuit and short-circuit test, we observed high resistance (from 10 to 15 Ω). Since the conductor loss for silver at 8 MHz is very small, most of the losses come from the material dielectric loss. As a result, the overall transformer performance for Prototype E is poor as compared to other Prototypes (A, B, C, and D). Smith chart plot of the input impedance of Transformer E with a 50 Ω load is shown in Figure 24. The ideal input impedance should be 12.5 Ω , the actual value observed around 8 MHz is 4 Ω . It is concluded that low-frequency transmission-line transformer is possible by using materials with a large dielectric constant. We are able to find commercially available material with dielectric constant over 1000, but the losses are too high for practical purpose. This bottleneck would only be overcome by the advance of material technology. With the available low-loss material, the transmission line transformer is most suitable for frequency around 100 MHz.

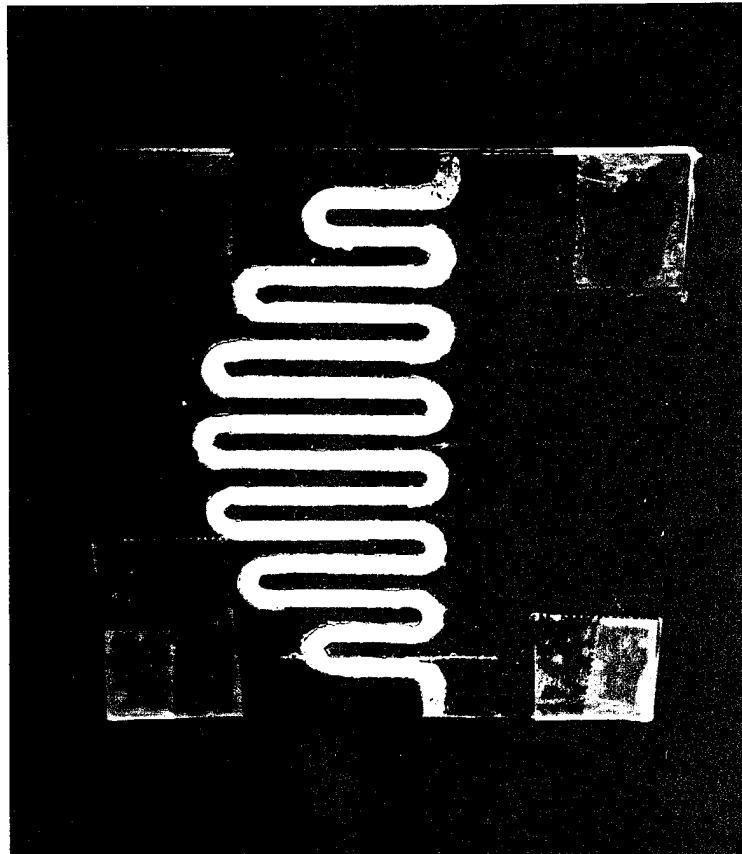


Figure 22. The Top View of the Prototype Transformer E.

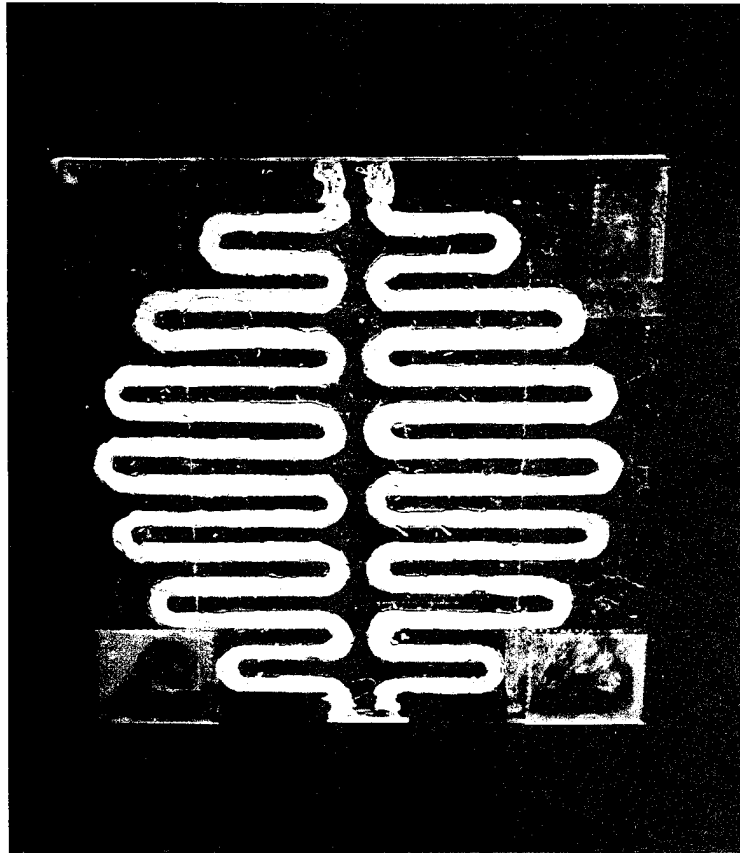
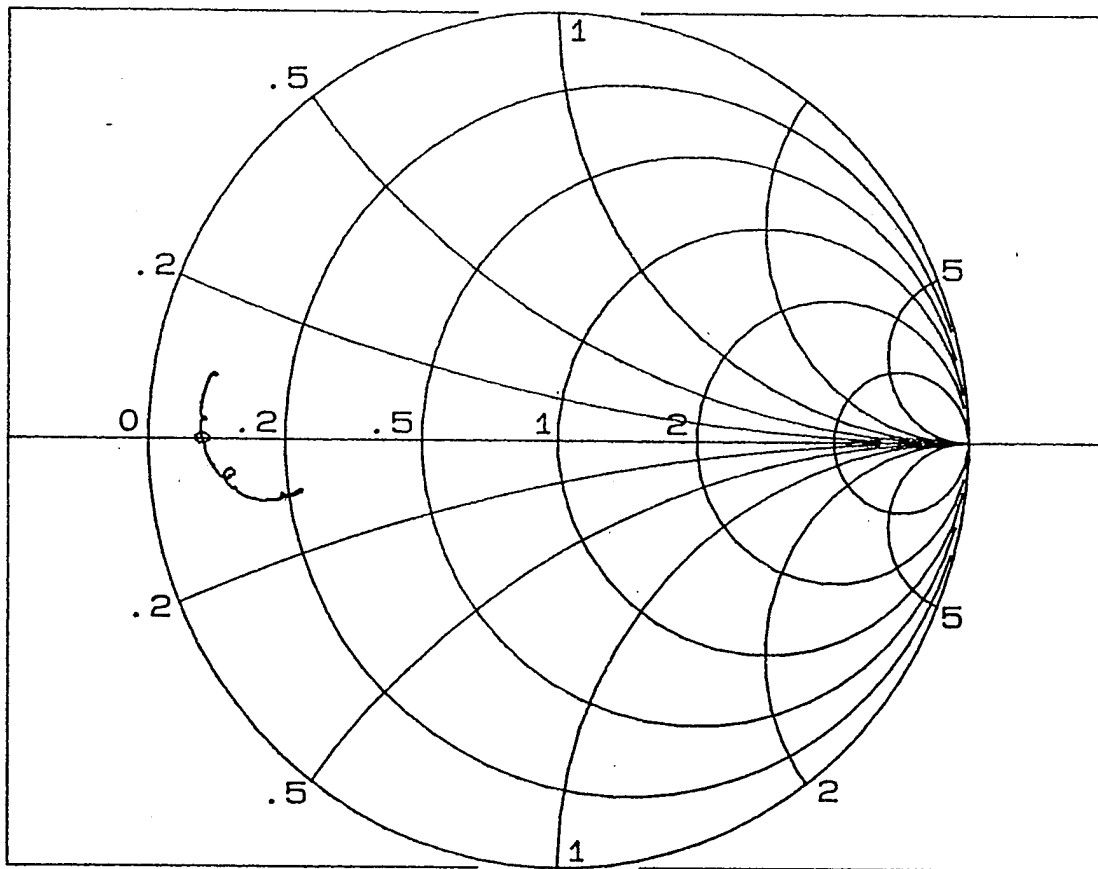


Figure 23. The Bottom View of the Prototype Transformer E.

FULL SCALE 1.0000
PHASE REF 0.0deg
REF POSN 0.0deg

MARKER 7 512 500.000Hz
Z MAG (S11) 71.986E-3
Z PHS (S11) 1.609deg



START 5 000 000.000Hz
AMPTD 15.0dBm

STOP 10 000 000.000Hz

Figure 24. Smith chart plot of the input impedance of the step-down (1 to 4) Transformer E with a 50Ω load.

IV. Conclusions

In this project, we proposed novel transformers for power supplies. The transformer consists of the cascade of sections of transmission lines, each a quarter-wave length long at the desired frequency. In the proposed transformers, ferrite core that is conventional used to confine magnetic flux and provide flux path is abandoned, and power conversion is through the propagation of electromagnetic waves instead of magnetic flux. There is basically no constraint on the frequency requirement and the type transmission line one can use.

For practical purpose, smaller components with equal or better performance are more desirable. The proposed transmission line transformers have the requirement that the each line length is a quarter of the transmission-line guided wave-length. Therefore, the proposed transformer is ideal for high frequency operation. For transformer with dimension in the order of centimeter, the ideal frequency is around 100 MHz.

Electronic devices on integrated circuit structures are most popular for their desirable features such as **low-profile, higher-density, small size and weight, low cost and high reliability**. Printed-circuit transformer can be an integrated part of a circuit board with other components. In this project, parallel strip lines sandwiching a printed circuit board were used as the transmission lines. Printed meandered striplines on a multi-layer structure were used to optimize the component size. A 50 MHz coaxial line transformer was first developed to verify the design concept. Three printed stripline transformers are built on Teflon-fiberglass with design frequencies, 100 MHz, 115 MHz, and 110 MHz, respectively. The dimension of the transformer is less than 4 cm. S parameter tests for a 50 ohm load show the measured transformer ratio agrees excellently with the prediction. We did not test the power handling capability and the overall efficiency due to the lack of high frequency power amplifier. The analysis of the loss mechanism shows that most of the power losses are due to conductor loss and the overall efficiency should be greater than 98%.

In order to lower transformer frequency without increase the overall dimension, a transformer is designed and built on a lead Zirconate Titanate material with dielectric constant 1100. The guided wavelength of the strip lines on such material at 8 MHz is reduced to about 1.6 meters. 40 cm quarter-wave strip lines are built on a 3.1 inch by 3.1 inch plate. Open-circuit and short-circuit tests on network analyzer show the actual quarter-wave length is at 8.3 MHz instead and the line impedance also agrees well with the design value. The S parameter measurement of the transformer ratio does not show good result. We found that although Titanate material provides good wavelength reduction, the material loss is very high. Material search for very low loss and large dielectric constant (>1000) continues. In the future, if this kind of materials becomes available, we will be able to develop low-frequency, high efficiency, high power, and low loss coreless transformers.

V. Bibliography

- [1]. J.G. Kassakian and M.F. Schlecht, "High-frequency high-density converters for distributed power supply systems," *Proceedings of IEEE*, Vol. 76, no. 4, pp. 362-376, April 1988.
- [2]. J.G. Kassakian, M.F. Schlecht, and G.C. Verghese, Principles of Power Electronics, Addison-Wesley Publishing Company, New York, 1991.
- [3]. J.A. Ferreira, Electromagnetic Modeling of Power Electronic Converters, Kluwer Academic Publishers, Boston, 1989.
- [4]. K.D.T. Ngo, R.P. Alley, A.J. Yerman, R.J. Charles, and M.H. Kuo, "Design issues for the transformer in a low-voltage power supply with high efficiency and high power density," *IEEE Trans. on Power Electronics*, vol. 7, no. 3, pp. 592-600, July 1992.
- [5]. M.A. Morrill, V.A. Caliskan, and C.Q. Lee, "High frequency planar power transformers," *IEEE Trans. on Power Electronics*, Vol. 7, no. 3, pp. 607-613, July 1992.
- [6]. D. van der Linde, A.A.M. Boon, and J.B. Klaassens, "Design of a high-frequency planar power transformer in multilayer technology," in *IEEE Trans. on Industrial Electronics*, vol. 38, no. 2, pp. 135-141, April 1991.
- [7]. K.D.T. Ngo, R.P. Alley, and A.J. Yerman, "Fabrication method for a winding assembly with a large number of planar layers," 1991 *Applied Power Electronics Conf. Proceedings*, pp. 543-549.
- [8]. G. Skutt, F.C. Lee, R. Ridley, and D. Nicol, "Leakage inductance and termination effects in a high-power planar magnetic structure," 1994 *Applied Power Electronics Conf. Proceedings*, pp. 295-301.
- [9]. M.H. Kheraluwala, D.W. Novotny, and D.M. Divan, "Design consideration for high power high frequency transformers," 1990 *Applied Power Electronics Conf. Proceedings*, pp. 734-743.
- [10]. A.F. Goldberg, J.G. Kassakian and M.F. Schlecht, "Issues related to 1-10 MHz transformer design," *IEEE trans. on Power Electronics*, Vol. 4, no. 1, pp. 113-123, January 1989.
- [11]. M.C. Smit, J.A. Ferreira, and J.D. Van Wyk, "Application of transmission line principles to high frequency power converters," *Power Electronics Specialists Conf. Rec.*, June 1992, pp. 1423-1430.

- [12]. M. Ehsani, O.H. Stielau, J.D. Van Wyk, and I.J. Pitel, " Integrated reactive components in power electronic circuits," *IEEE Trans. on Power Electronics*, vol. 8, no. 2, pp. 209-215, April, 1993.
- [13]. C.L. Ruthroff, "Some broad-band transformers," In *Proc. IRE*, vol. 47, pp. 1337-1342, 1959.
- [14]. G. Oltman, "The compensated balun," *IEEE Trans. on Microwave Theory and Techniques*, pp. 112-119, March 1966.
- [15]. Robert E. Collin, Foundation for Microwave Engineering, *McGraw-Hill Publishing Company*, 1992.
- [16]. C.W. Allen and H.L. Krauss, "Wide-band rotary transformer- unbalanced current analysis," *Proceedings of the IEEE*, vol. 65, no. 2, pp. 200-206, February 1977.
- [17]. T. Itoh, Planar Transmission Line Structures, *IEEE Press* 1987.
- [18]. R.K. Hoffmann, Handbook of Microwave Integrated Circuits, *Artech House*, 1987
- [19]. S.R. Seshadri, Fundamentals of Transmission Lines and Electromagnetic Fields, *Addison-Wesley, Reading, Massachusetts*, 1971.